11th World Congress on Computational Mechanics (WCCM XI)
5th European Conference on Computational Mechanics (ECCM V)
6th European Conference on Computational Fluid Dynamics (ECFD VI)
E. Oñate, J. Oliver and A. Huerta (Eds)

# A NURBS BASED COLLOCATION APPROACH FOR SB-FEM

**LIN CHEN*, WOLFGANG DORNISCH* AND SVEN KLINKEL***

* Lehrstuhl für Baustatik und Baudynamik
RWTH Aachen University
Mies-van-der-Rohe-Str. 1, 52074 Aachen, Germany
e-mail: lin.chen@lbb.rwth-aachen.de, web page: http://www.lbb.rwth-aachen.de/

**Key words:** Scaled boundary finite element method, Isogeometric collocation method, NURBS basis functions, Body forces, Stiffness matrix

**Abstract.** The paper is concerned with a new numerical method to solve the in-plane motion problem of elastic solids. An element formulation is derived, which is based on the so-called scaled boundary finite-element method (SB-FEM). In the procedure, only the boundary of the element is discretized. The domain inside the element is described by a radial scaling factor. Applying the weak form in circumferential direction, the governing partial differential equations of elasticity are transformed to the scaled boundary finite element equation, where the unknown displacements are a function of the radial scaling factor. To solve this equation, the isogeometric collocation method is employed. It is directly applied to the strong form of the equation with a finite-dimensional space of candidate solutions (NURBS basis functions) and a number of collocation points. Then, a linear system of equations is attained, which can be solved with common solvers. This procedure is used to evaluate the displacements of a cantilever beam. Comparisons with the analytical solution are presented. Very promising results are obtained, which demonstrates that the method is stable, robust, higher-order accurate and efficient.

## 1 INTRODUCTION

Recently, in solids mechanics, a novel semi-analytical procedure called the scaled boundary finite-element method (SB-FEM) has been developed, which is a fundamental-solution-less boundary element method based on finite elements. In this approach, only the boundary of the analysis domain is discretized. The fundamental solution is not needed in the analysis, see [1, 2]. Standard finite element methods are employed to represent the geometry and the displacements of the boundary. Several applications in different fields, such as wave propagation [3], structural analysis [4, 5] and fracture mechanics [6] were addressed. The derivation of the fundamental equations of SB-FEM was presented

in various publications [1, 2]. The readers can find the detailed theoretical derivations of the method in the aforementioned contributions. In general, the essence of SB-FEM is the derivation of the scaled boundary finite element equation (SB-FEE). The common solution procedure for this equation is based on the eigenvalue method, see e.g. [7, 8]. The displacement field is formulated as a power series in terms of the radial scaling parameter. The eigenvalues determine the powers of the terms in the series. The corresponding eigenvectors describe the angular variations. However, present eigenvalue solving methods require additional treatments for multiple eigenvalues with parallel eigenvectors. It results in logarithmic terms in the solutions, which deteriorates the accuracy of the method, see [4]. An additional approach to solve the SB-FEE is the matrix function solution [4], which is based on the theory of matrix functions and the real Schur decomposition. In the analysis, it is not necessary to employ the logarithmic functions in the solution. It is possible to simulate the stress fields with logarithmic singularity. However, the Schur decomposition is not unique for the square matrix.
In the present paper the isogeometric collocation method will be employed to solve the SB-FEE. Isogeometric analysis (IGA) [9] employs the basis functions for the description of the geometry in the design process also for the structural analysis. Thus, in the analysis process, it is ensured that the geometry is represented exactly. Different types of geometry descriptions can be used, we restrain ourselves to non-uniform rational B-splines (NURBS) in the following. The higher continuity provided by NURBS allows to use collocation of the strong form of the equation instead of using the Galerkin method for the weak form. It is more efficient than Galerkin based schemes [10]. A finite-dimensional space of candidate solutions (NURBS basis functions) and a number of points - called collocation points - are constructed. The solutions, which satisfy the given equation at the collocation points, are selected. If a certain set of collocation points is used, the method is numerically stable [11]. For the implementation in the present study, the SB-FEE is evaluated at all collocation points, and assembled to a system of linear equations. A standard linear solver is used. This procedure is used to evaluate the displacements of a cantilever beam. Comparisons between the proposed approach and the analytical solutions are presented.

## 2 Scaled boundary finite element method

In the finite element method, the motion equations of a single element are firstly derived which leads to its static stiffness matrix and mass matrix. Assembling all finite elements and enforcing equilibrium and compatibility, it yields the equations of motion in the global system with its corresponding property matrices. The derivation of SB-FEM is analogous. The details of the method can be found in the work of Song and Wolf [1, 2]. Here, only the application of the method in the present study will be addressed.
For the sake of illustration, the linear analysis of a bounded domain (Fig.1a) in elastostatics is addressed. In the domain, the body forces $\mathbf{p}$ are applied. On the boundary, the displacement $u$ on $B_u$, surface tractions $t$ on $B_t$ and nodal forces $\mathbf{F}$ are prescribed. Analogous to the standard finite element method, the domain $V$ is discritzied into finite

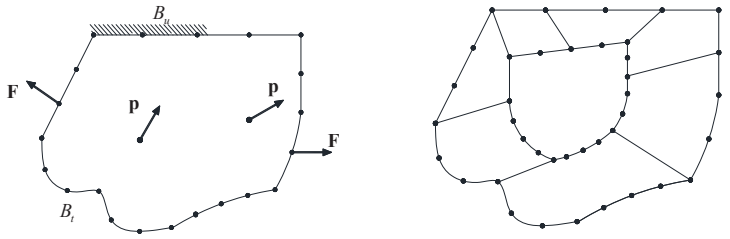


(a) Analysis domain (b) Discretization of the domain

**Figure 1**: Problem definition and discretization of the medium with finite elements

elements (Fig.1b). It is very flexible to define the finite elements. There is no restriction on the geometry and the number of nodes of each element. The analysis is firstly carried out on each element to obtain its stiffness matrix and nodal forces due to the body forces.

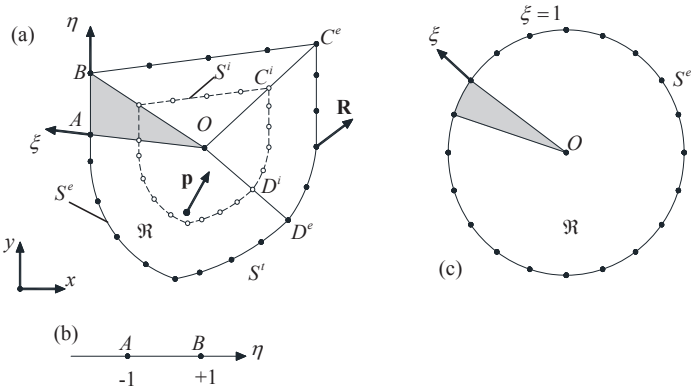


**Figure 2**: Two-dimensional elastic element: (a) scaled boundary coordinates; (b) two nodes line element and (c) isoperimetric surface.

Considering a two-dimensional elastic element $\Re$ from Fig.1b (See Fig.2), a scaling center $O$ is chosen in a zone from which the total boundary of the element is visible. Here, the scaling center $O$ is employed to describe the whole element, which will be addressed in detail later. The Cartesian coordinate system $(x, y)$ is set as shown in Fig.2. $(x_0, y_0)$ is introduced to denote the scaling center $O$, as the coordinates $(\bar{x}, \bar{y})$ are reserved for the boundary of the element. The body forces $\mathbf{p}$ are presented inside the element. The nodal forces $\mathbf{R}$ at each node of the element and surface tractions $\mathbf{t}$ on the boundary of the element are prescribed. In addition, two local coordinates are defined to describe the element. One is the curvilinear coordinate $\eta$ in the circumference along the direction of the element boundary; while another one is the radial coordinate $\xi$ pointing from the scaling center $O$ to a point on the element boundary, $\xi = 0$ in $O$ and $\xi = 1$ on the boundary of the element are chosen. This is similar to the isoparametric concept in the finite element method; the corresponding isoparametric surface is shown in Fig.2c. By

scaling the element boundary in the radial direction with respect to $O$, the whole element is covered, which means the geometry of the element can be defined by the radial coordinate $\xi$ (with $0 \leq \xi \leq 1$) and $\eta$. When $\xi = 1$, the element boundary $S^e$ (superscript 'e' for element) is defined (Fig.2a). When $\xi < 1$, with the scaling strategy, the element boundary $S^e$ will zoom out to inner boundary $S^i$ (superscript '$i$' for inside element) (Fig.2a).
In the derivation, the standard finite element is employed to discretize the element boundary $S^e$. As described before, the curvilinear coordinate $\eta$ is used to parameterize it. In the present study, finite elements with two nodes are employed. To distinguish it from the parent element $\Re$ in Fig.2a, it is called sub-element. A typical curved line sub-element $AB$ on part of the boundary $S^e$ is shown in Fig.2b with the parameterization coordinate $\eta$. Scaling the sub-element $AB$ with respect to $O$, a shaded triangular area $OAB$ will be observed (See Fig.2a). Inside the element $\Re$, the nodes on the inner boundary $S^i$, such as nodes $C^i$ and $D^i$ here, can be obtained by scaling the nodes $C^e$ and $D^e$ from $S^e$ (Fig.2a). For the element $\Re$, applying the weak form in circumferential direction, the governing partial differential equations of elasticity are transformed to the scaled boundary finite element equation (SB-FEE), which is a non-homogenous ordinary differential equation of Euler type. In the equation, the unknowns are nodal displacements of the boundary $S^i$ and $S^e$. The final equations are expressed as follows [7]:

$$\xi^2 \mathbf{K}_{11} \bar{\mathbf{U}}(\xi)_{,\xi\xi} + \xi \left(\mathbf{K}_{12} - \mathbf{K}_{21} + \mathbf{K}_{11}\right) \bar{\mathbf{U}}(\xi)_{,\xi} - \mathbf{K}_{22} \bar{\mathbf{U}}(\xi) + \mathbf{F}(\xi) = 0 \tag{1}$$

where $\bar{\mathbf{U}}(\xi)$ represents the nodal displacement of the boundary $S^i$ (Fig.2a). It reads

$$\bar{\mathbf{U}}(\xi) = \left\{ \begin{array}{cccc} \bar{\mathbf{U}}_1(\xi) & \bar{\mathbf{U}}_2(\xi) & \ldots & \bar{\mathbf{U}}_{m-1}(\xi) \quad \bar{\mathbf{U}}_m(\xi) \end{array} \right\}^T \tag{2}$$

with the nodal values $\bar{\mathbf{U}}_i(\xi) = \left\{ \begin{array}{cc} \bar{U}_{ix}(\xi) & \bar{U}_{iy}(\xi) \end{array} \right\}^T$, where $m$ is the number of nodes on the boundary $S^i$. This number is identical to the number of nodes on the boundary $S^e$ due to the scaling effect. The abbreviation $(\cdot)_{,\xi} = \partial(\cdot)/\partial\xi$ holds,. Analogously $(\cdot)_{,i}$ is defined.
The coefficient matrices $\mathbf{K}_{11}$, $\mathbf{K}_{12}$, $\mathbf{K}_{21}$ and $\mathbf{K}_{22}$ are defined on the boundary $S^e$. They are obtained by assembling the corresponding matrices of each sub-element on the boundary $S^e$ (Fig.2a) as in the standard finite element method [4]. Thus, it is significant to calculate the coefficient matrices of the sub-element. To simplify the nomenclature, the same symbols of the coefficient matrices are used for the final assembled matrices and for the matrices of the sub-element. Here, the coefficient matrices of the sub-element $AB$ in Fig.2b will be presented for illustration [12]

$$\begin{aligned} \mathbf{K}_{11} &= \int_{-1}^{1} \mathbf{B}_1(\eta)^T \mathbf{D} \mathbf{B}_1(\eta) \left|J(\eta)\right| d\eta \qquad & \mathbf{K}_{12} &= \int_{-1}^{1} \mathbf{B}_1(\eta)^T \mathbf{D} \mathbf{B}_2(\eta) \left|J(\eta)\right| d\eta \\ \mathbf{K}_{21} &= \int_{-1}^{1} \mathbf{B}_2(\eta)^T \mathbf{D} \mathbf{B}_1(\eta) \left|J(\eta)\right| d\eta \qquad & \mathbf{K}_{22} &= \int_{-1}^{1} \mathbf{B}_1(\eta)^T \mathbf{D} \mathbf{B}_1(\eta) \left|J(\eta)\right| d\eta \end{aligned} \tag{3}$$

where $D$ is the elasticity matrix. Any general anisotropic material can be used. For example, the elasticity matrix of a plane stress linear isotropic material is:

$$\mathbf{D} = \frac{E}{1-\nu^2}\begin{bmatrix} 1 & \nu & 0 \\ \nu & 1 & 0 \\ 0 & 0 & (1-\nu)/2 \end{bmatrix} \tag{4}$$

The matrices $\mathbf{B}_1(\eta)$ and $\mathbf{B}_2(\eta)$ in the integrand can be obtained as shown in [12] by

$$\mathbf{B}_1(\eta) = \tfrac{1}{|J(\eta)|}\mathbf{b}_1(\eta)\,\mathbf{N}(\eta) \qquad \mathbf{B}_2(\eta) = \tfrac{1}{|J(\eta)|}\mathbf{b}_2(\eta)\,\mathbf{N}(\eta)_{,\eta} \tag{5}$$

in which $N(\eta)$ is any general shape functions matrix. In the present study it is expressed by

$$\mathbf{N}(\eta) = \begin{bmatrix} (1-\eta)/2 & 0 & (1+\eta)/2 & 0 \\ 0 & (1-\eta)/2 & 0 & (1+\eta)/2 \end{bmatrix}. \tag{6}$$

In Eqs. (3) and (5), $|J(\eta)|$ is the determination of the Jacob matrix $\mathbf{J}(\eta)$, which is defined by

$$\mathbf{J}(\eta) = \begin{bmatrix} \bar{x} - x_0 & \bar{y} - y_0 \\ \bar{x}_{,\eta} & \bar{y}_{,\eta} \end{bmatrix}, \tag{7}$$

where $(\bar{x}, \bar{y})$ are the coordinates of the point on the sub-element $AB$, which is approximated by the standard finite element method yielding

$$\begin{pmatrix} \bar{x} \\ \bar{y} \end{pmatrix} = \mathbf{N}(\eta)\left(\bar{x}_A, \bar{y}_A, \bar{x}_B, \bar{y}_B\right)^T. \tag{8}$$

The coordinate of points inside the shaded triangular area $OAB$ (Fig.2a) are obtained by

$$\begin{pmatrix} x \\ y \end{pmatrix} = \begin{pmatrix} x_0 \\ y_0 \end{pmatrix} + \xi\left(\mathbf{N}(\eta)\left(\bar{x}_A, \bar{y}_A, \bar{x}_B, \bar{y}_B\right)^T - \begin{pmatrix} x_0 \\ y_0 \end{pmatrix}\right). \tag{9}$$

The matrices $\mathbf{b}_1(\eta)$ and $\mathbf{b}_2(\eta)$ in Eq. (5) read

$$\mathbf{b}_1(\eta)^T = \begin{bmatrix} \bar{y}_{,\eta} & 0 & -\bar{x}_{,\eta} \\ 0 & -\bar{x}_{,\eta} & \bar{y}_{,\eta} \end{bmatrix} \qquad \mathbf{b}_2(\eta)^T = \begin{bmatrix} -\bar{y} & 0 & \bar{x} \\ 0 & \bar{x} & -\bar{y} \end{bmatrix}. \tag{10}$$

As the integrations over the sub-element $AB$ are regular, the standard numerical techniques in the finite element method, such as Gauss-Legendre quadrature method, are directly applicable in Eq. (1).
The vector $\mathbf{F}(\xi)$ in Eq. (1) is the contribution from the body forces and tractions [13]

$$\mathbf{F}(\xi) = \xi^2\mathbf{F}^b(\xi) + \xi\mathbf{F}^t(\xi), \tag{11}$$

where $\mathbf{F}^b(\xi)$ is the contribution of the body force $\mathbf{p}(\xi)$ with $\mathbf{p}(\xi) = \begin{bmatrix} p_x(\xi) & p_y(\xi) \end{bmatrix}^T$. $\mathbf{F}^t(\xi)$ is the contribution of the prescribed surface tractions $\mathbf{t}(\xi) = \begin{bmatrix} t_x(\xi) & t_y(\xi) \end{bmatrix}^T$. In

order to obtain $\mathbf{F}(\xi)$, akin to the calculation of $\mathbf{K}_{11}$, the corresponding vector of each sub-element should be calculated firstly, and then assembled. The stress-displacement relationships reads

$$\boldsymbol{\sigma}(\xi,\eta) = \mathbf{D}\left(\mathbf{B}_1(\eta)\,\bar{\mathbf{U}}(\xi)_{,\xi} + \frac{1}{\xi}\mathbf{B}_2(\eta)\,\bar{\mathbf{U}}(\xi)\right), \tag{12}$$

see [12]. Here, $\mathbf{B}_1(\eta)$ and $\mathbf{B}_2(\eta)$ are assembled matrices of all sub-elements on the boundary $S^e$. According to [13] the internal nodal forces on the inner boundary $S^i$ (constant $\xi$) are equal to

$$\mathbf{q}(\xi) = \xi\mathbf{K}_{11}\bar{\mathbf{U}}(\xi)_{,\xi} + \mathbf{K}_{12}\bar{\mathbf{U}}(\xi) \tag{13}$$

where $\mathbf{q}(\xi) = \left\{ \begin{array}{cccccc} \mathbf{q}_1(\xi) & \mathbf{q}_2(\xi) & \dots & \mathbf{q}_{m-1}(\xi) & \mathbf{q}_m(\xi) \end{array} \right\}^T$ denotes the internal nodal forces of the inner boundary $S^i$ (Fig.2a) and $\mathbf{q}_i(\xi)$ $(i = 1, 2, ...., m)$ are the internal forces of node $i$ with $\mathbf{q}_i(\xi) = \left\{ \begin{array}{cc} q_{ix}(\xi) & q_{iy}(\xi) \end{array} \right\}^T$ with $m$ being the number of nodes on the boundary $S^i$.

For the nodal forces $\mathbf{R}$ on the boundary $S^e$ of the element $\Re$ $(\xi = 1)$, it holds $\mathbf{R} = \mathbf{q}(\xi = 1)$. The stiffness matrix $\mathbf{K}$ of the element $\Re$ relating the nodal forces $\mathbf{R}$ and nodal displacements $\bar{\mathbf{U}}$ on the boundary $S^e$ of the element $(\xi = 1)$ is defined as

$$\mathbf{R} = \mathbf{q}(\xi = 1) = \mathbf{K}\bar{\mathbf{U}}(\xi = 1) - \mathbf{R}^F, \tag{14}$$

where $\mathbf{R}^F$ denotes the nodal forces due to body forces and surface tractions of the element.

## 3 Solution procedure for the scaled boundary finite element equation

The present common solution procedure for the scaled boundary finite element equation (SB-FEE) is based on the eigenvalue method [8] and the matrix function solution [4]. However, there are some restrictions existing in both approaches. Thus, in the present study, the isogeometric collocation method is employed to solve the SB-FEE, which is introduced in Ref. [11] to solve differential equations. It has been proved to be numerically stable [11]. In isogeometric analysis, both the geometry and the unknown variables are discretized with the same basis functions. Here Non-uniform Rational B-Splines (NURBS) are used. NURBS are smooth approximating functions constructed by piecewise polynomials. To define such functions, a knot vector as a set of non-decreasing real numbers representing coordinates in the parametric space is introduced

$$\Xi = \{\xi_1 = 0, ...., \xi_{n+p+1} = 1\} \tag{15}$$

where $p$ denotes the order of NURBS and $n$ is the number of basis functions (and control points). For the present study one knot span with $p$-refinement is used. This has inherently benefits for the isogeometric collocation method due to the radial coordinate being defined in $0 \leq \xi \leq 1$. Thus, coordinate transformation is not necessary. The analysis can directly be carried out with the radial coordinate $\xi$, which means the radial coordinate $\xi$

represents the parametric space in the isogeometric analysis. The knot values $\xi = 0$ and $\xi = 1$ denote the scaling center $O$ and the boundary $S^e$ of the element $\Re$.
In order to construct the NURBS basis functions, B-splines basis function are computed with the Cox–De Boor formula

$$\begin{aligned} p = 0 : \quad & N_{i,0}(\xi) = \begin{cases} 1 & \text{if } \bar{\xi}_i \leq \xi \leq \bar{\xi}_{i+1} \\ 0 & \text{otherwise} \end{cases} \\ p > 0 : \quad & N_{i,p}(\xi) = \frac{\xi - \bar{\xi}_i}{\bar{\xi}_{i+p} - \bar{\xi}_i} N_{i,p-1}(\xi) + \frac{\bar{\xi}_{i+p+1} - \xi}{\bar{\xi}_{i+p+1} - \bar{\xi}_{i+1}} N_{i+1,p-1}(\xi) \ , \end{aligned} \tag{16}$$

in which the specific convention $0/0 = 0$ is introduced. Then, the NURBS basis functions of order $p$ are defined as

$$R_{i,p}(\xi) = \frac{N_{i,p}(\xi)\,\omega_i}{\sum_{j=1}^{n} N_{j,p}(\xi)\,\omega_j} \,, \tag{17}$$

where $\omega_i (i = 1, 2, ...., n)$ denotes the weight of the $i-$th basis functions. Obviously, when all the weights of the NURBS basis functions are equal, the NURBS basis functions will reduce to the B-splines basis functions. Therefore, B-splines are a special case of NURBS. The $k$th derivative with respect to $\xi$ is given as

$$\frac{d^k}{d\xi^k} R_{i,p}(\xi) = \frac{p}{\xi_{i+p} - \xi_i} \left( \frac{d^{k-1}}{d\xi^{k-1}} R_{i,p-1}(\xi) \right) - \frac{p}{\xi_{i+p+1} - \xi_{i+1}} \left( \frac{d^{k-1}}{d\xi^{k-1}} R_{i+1,p-1}(\xi) \right) . \tag{18}$$

Within an isogeometric framework, the radial coordinate $\xi$ and the displacement $\bar{U}(\xi)$ in the element $\Re$ are approximated by NURBS basis functions as

$$\xi = \sum_{i=1}^{n} R_{i,p}(\xi)\,\bar{\xi}_i \qquad \bar{\mathbf{U}}(\xi)^h = \sum\nolimits_{i=1}^{n} R_{i,p}(\xi)\,\bar{\mathbf{U}}\big(\bar{\xi}_i\big)^c \,, \tag{19}$$

where $\bar{\mathbf{U}}\big(\bar{\xi}_i\big)^c \ (i = 1, 2, ...., n)$ are the unknown control variables; $\bar{\xi}_i$ are the coordinates of the control points, which are obtained by the Greville abscissae due to the specificity of the present analysis (1D case with $p$-refinement):

$$\bar{\xi}_i = \frac{\xi_{i+1} + \xi_{i+2} + .... + \xi_{i+p}}{p} \qquad (i = 1, 2, ...., n) \tag{20}$$

Due to the property of the $p$-refinement, $\bar{\xi}_1 = 0$ and $\bar{\xi}_n = 1$ holds.
With these approximations, SB-FEE (Eq.(1)) is collocated at the images of the Greville abscissae $\bar{\xi}_i$ excluding the force boundary of the element $\Re$. This can be formally started by employing Eq.(1), (13) and (14):

$$\bar{\xi}_i^2 \mathbf{K}_{11} \bar{\mathbf{U}}\left(\bar{\xi}_i\right)_{,\xi\xi}^{h} + \bar{\xi}_i \left(\mathbf{K}_{12} - \mathbf{K}_{21} + \mathbf{K}_{11}\right) \bar{\mathbf{U}}\left(\bar{\xi}_i\right)_{,\xi}^{h} - \mathbf{K}_{22} \bar{\mathbf{U}}\big(\bar{\xi}_i\big)^h + \mathbf{F}\left(\bar{\xi}_i\right) = 0 \quad (i = 1, 2, ...., n-1) \tag{21}$$

$$\bar{\xi}_n \mathbf{K}_{11} \bar{\mathbf{U}}\left(\bar{\xi}_n\right)_{,\xi}^{h} + \mathbf{K}_{12} \bar{\mathbf{U}}\big(\bar{\xi}_n\big)^h = \mathbf{R} \tag{22}$$

Combining Eqs.(21) and (22) results in a system of linear algebraic equations

$$\begin{bmatrix} \mathbf{T}_{11} & \mathbf{T}_{12} & \cdots & \mathbf{T}_{1n} \\ \mathbf{T}_{21} & \mathbf{T}_{22} & \cdots & \mathbf{T}_{2n} \\ \vdots & \vdots & \cdots & \vdots \\ \mathbf{T}_{n1} & \mathbf{T}_{n2} & \cdots & \mathbf{T}_{nn} \end{bmatrix} \begin{Bmatrix} \bar{\mathbf{U}}\left(\bar{\xi}_1\right)^c \\ \bar{\mathbf{U}}\left(\bar{\xi}_2\right)^c \\ \vdots \\ \bar{\mathbf{U}}\left(\bar{\xi}_n\right)^c \end{Bmatrix} = \begin{Bmatrix} -\mathbf{F}\left(\bar{\xi}_1\right) \\ -\mathbf{F}\left(\bar{\xi}_2\right) \\ \vdots \\ \mathbf{R} \end{Bmatrix}, \tag{23}$$

where $\mathbf{T}_{ij}\,(i,j=1,2,....,n)$ is the coefficient matrix in Eq.(21) and (22). The matrix has the size $2m\times 2m$ with $m$ being the number of the nodes used to approximate the boundary $S^e$ and $S^i$. The vector $\mathbf{F}\left(\bar{\xi}_i\right)$ $(i=1,2,....,n-1)$ can be obtained from Eq. (11). If $\bar{\xi}_1=0$ is employed in Eq. (21) then numerical instability will arise. In order to eliminate this, the value of $\bar{\xi}_1$ is slightly increased to move the collocation point out of the center. In the present study $\bar{\xi}_1=0.01$ is used.
Further, Eq.(23) can be written in portioned form as

$$\begin{bmatrix} \mathbf{\Gamma}_{11} & \mathbf{\Gamma}_{12} \\ \mathbf{\Gamma}_{21} & \mathbf{\Gamma}_{22} \end{bmatrix} \begin{Bmatrix} \mathbf{\Psi} \\ \bar{\mathbf{U}}\left(\bar{\xi}_n\right)^c \end{Bmatrix} = \begin{Bmatrix} \mathbf{\Omega} \\ \mathbf{R} \end{Bmatrix}, \tag{24}$$

where $\mathbf{\Psi} = \left\{ \begin{array}{ccccc} \bar{\mathbf{U}}\left(\bar{\xi}_1\right)^c & \bar{\mathbf{U}}\left(\bar{\xi}_2\right)^c & \cdots & \bar{\mathbf{U}}\left(\bar{\xi}_{n-1}\right)^c \end{array} \right\}^T$ and other matrices can be easily inferred. From Eq.(24), the following expression can be obtained

$$\mathbf{R} = \left(\mathbf{\Gamma}_{22} - \mathbf{\Gamma}_{21}{\mathbf{\Gamma}_{11}}^{-1}\mathbf{\Gamma}_{12}\right)\bar{\mathbf{U}}\left(\bar{\xi}_n\right)^c + \mathbf{\Gamma}_{21}{\mathbf{\Gamma}_{11}}^{-1}\mathbf{\Omega}\,. \tag{25}$$

Here, based on Eq. (20), it implies $\bar{\mathbf{U}}\left(\bar{\xi}_n\right)^c = \bar{\mathbf{U}}\left(\xi=1\right)$. Comparing with Eq. (14), the stiffness matrix of the element $\Re$ can be obtained by

$$\mathbf{K} = \mathbf{\Gamma}_{22} - \mathbf{\Gamma}_{21}{\mathbf{\Gamma}_{11}}^{-1}\mathbf{\Gamma}_{12}\,. \tag{26}$$

Furthermore, the nodal loads $\mathbf{R}^F$ due to body forces and non-zero surface tractions are

$$\mathbf{R}^F = -\mathbf{\Gamma}_{21}{\mathbf{\Gamma}_{11}}^{-1}\mathbf{\Omega}\,. \tag{27}$$

Like in the finite element method, assembling the stiffness matrix and nodal loads $\mathbf{R}^F$ of all finite elements and enforcing equilibrium and compatibility, it yields the equation of motion in the global system. The corresponding displacements $\bar{\mathbf{U}}\left(\bar{\xi}_n\right)^c = \bar{\mathbf{U}}\left(\xi=1\right)$ on the boundary of each element are the results of solving Eq. (24) . Substituting $\bar{\mathbf{U}}\left(\bar{\xi}_n\right)$ into Eq. (25), the corresponding nodal loads $\mathbf{R}$ can be obtained. Also, the unknown displacements $\bar{\mathbf{U}}_i^c$ $(i=1,2,....,n-1)$ of each element can be derived with

$$\mathbf{\Psi} = {\mathbf{\Gamma}_{11}}^{-1}\left(\mathbf{\Omega} - \mathbf{\Gamma}_{12}\bar{\mathbf{U}}\left(\bar{\xi}_n\right)\right)\,, \tag{28}$$

where $\mathbf{\Psi}$ is the vector of the unknown displacements defined in Eq. (24).

Substituting $\bar{\mathbf{U}}\left(\bar{\xi}_n\right)$ and Eq. (28) into (19), the displacement $\bar{\mathbf{U}}(\xi)$ of each element can be obtained. The displacement $\mathbf{U}(\xi,\eta)$ inside each element can be calculated as [13]:

$$\mathbf{U}(\xi,\eta) = \mathbf{N}(\eta)\,\bar{\mathbf{U}}(\xi) \tag{29}$$

The stress $\boldsymbol{\sigma}(\xi,\eta)$ inside each element can be obtained by substituting Eq. (19) into Eq. (12). Here, the displacement $\mathbf{U}(\xi,\eta)$ and stress $\boldsymbol{\sigma}(\xi,\eta)$ are defined in the local coordinate system $(\xi,\eta)$. The corresponding values in the global coordinate system $(x,y)$ are obtained by the coordinate transformation from Eq. (9).

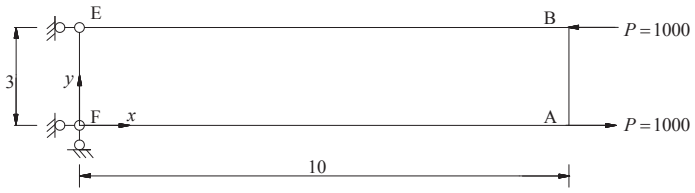


**Figure 3**: Cantilever beam under pure bending moment

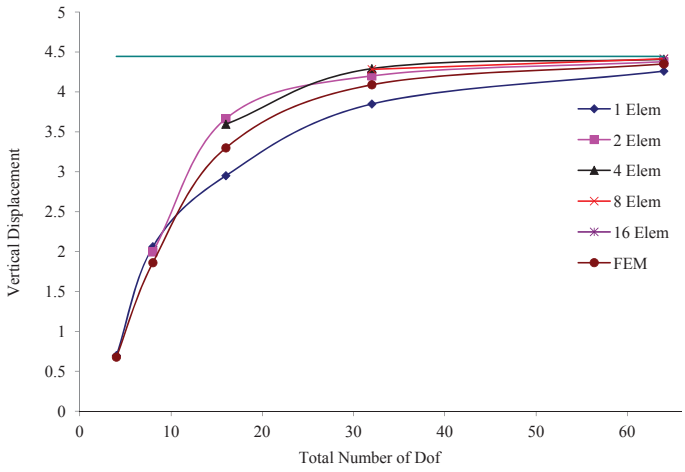


**Figure 4**: Vertical displacement at point A of the cantilever beam

## 4 Numerical example

In order to verify the theory, calculations were performed for a cantilever beam (Fig.3). Pure bending moment $M = 3P$ is exerted at the end of the beam. The properties of the beam are: Young's modulus $E = 15000$, thickness $d = 1$ and Poisson's ratio $\mu = 0.0$. Fig.3 shows the diagram in which the vertical displacement $v_A$ at point A is plotted versus the total number of degree-of-freedom in the calculation. In the analysis, the beam is equally

discretized by rectangular elements along $x$-direction. In $y$-direction, one element through the thickness is employed. The total number of nodes, employed in the discretization, is 4, 6, 10, 18 and 34 nodes, respectively, which are uniformly distributed at the boundary AF and BE. For example, if 4 nodes are employed, there are 2 nodes on the boundary AF and BE separately. For such amount of nodes, the maximum number of elements is 16 with 4 nodes per element. Since there is no restriction of the number of nodes per element in the proposed approach, we examined one element with different number of nodes. For example, when the beam is only modeled by one element, there could be with 4, 6, 10, 18 and 34 nodes on the element. Analogously, if the beam is discretized by 2 elements, the number of nodes per element could be 4, 6, 10 and 18 nodes, correspondingly. Also, for better illustration, comparison with standard finite element method (FEM) with the 4-node quadrilateral plane element (linear shape functions) is made. In FEM, the beam is only discretized along $x$-direction. In $y$-direction, only one element is used through the height. Thus, we could have 1, 2, 4, 8 and 16 elements with 4, 6, 10, 18 and 34 nodes, respectively. The results of the proposed method converge to the exact solution with increasing number of elements and nodes (See Fig.4). In general, the solutions of standard finite element method (FEM) are less accurate compared to those of the proposed approach. One could have results almost identical to those of FEM by discretizing the beam with one element in the present study.

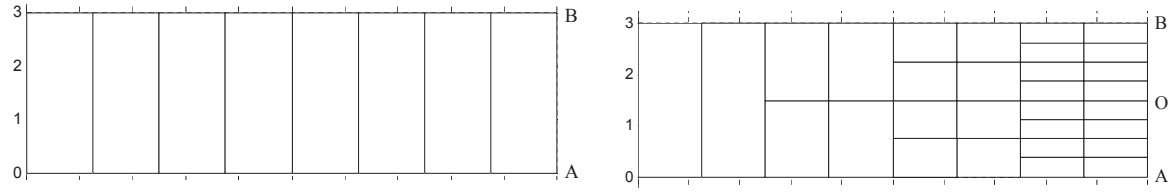


(a) 16 elements (b) 15 major elements plus 10 sub-elements

**Figure 5**: Dicretization of the beam

Next, in order to illustrate the proficiency of the proposed approach, the cantilever beam in Fig.3 is employed. The beam is firstly divided by 8 elements with 4-node quadrilateral plane elements (See Fig.5a), which is termed as 'initial mesh'. For such discretization, the displacement at the boundary AB is linear. However, the real displacement distribution at AB is non-linear. To represent it, the beam is further discretized by several quadrilateral plane sub-elements (See Fig.5b), which is termed as 're-mesh'. The deflection of boundary AB with respect to the neutral point O is shown in Fig.6. It can be observed that the boundary AB is non-linearly deflected, which implies that the proposed approach can easily obtain more accurate solutions by refining one element with many sub-elements without adding new calculation effort. It is worth noting that such ability of element refinement allows local refinement at concentration problem in solids mechanics. Also, it is interesting to note that the standard finite element method (FEM) cannot deal with

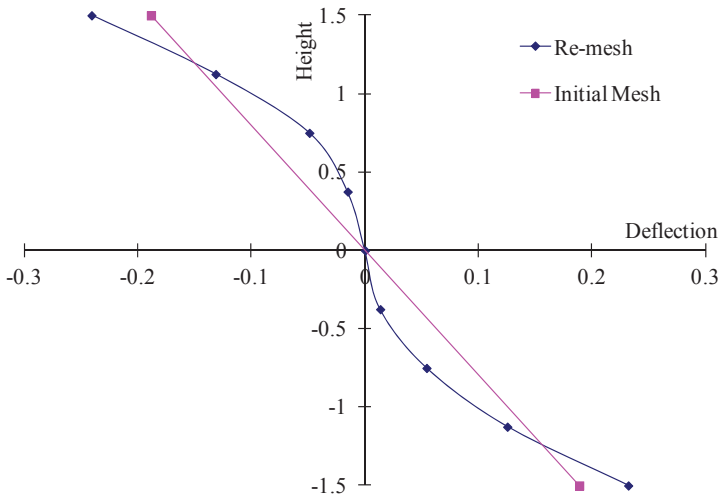


**Figure 6**: Deflection of boundary AB

this type of discretization in Fig.5b.

## 5 Conclusions

In this paper, a new numerical method is proposed to solve the in-plane motion problem of elastic solids. A novel element formulation is derived, which is based on the scaled boundary finite element method (SB-FEM) and isogeometric collocation method. In the procedure, the analysis domain is discretized to finite elements. The calculation is firstly performed to obtain the stiffness matrix of each element and the nodal forces due to body forces. In the implementation, SB-FEM is employed to transform the governing partial differential equations of elasticity to the so-called scaled boundary finite element equation, which is a non-homogenous ordinary differential equation of Euler type for the displacements. In order to solve it, the isogeometric collocation method is employed. The SB-FE equation is evaluated at all collocation points, assembled to a system of linear algebraic equations and solved. Displacements and stresses can be computed. The numerical examples demonstrate, that the procedure is stable, robust, higher-order accurate and efficient. Further applications of this approach can be extended to trimmed-NURBS, because the boundary-oriented character of SB-FEM ideally corresponds to the trimming of elements with NURBS curves, which is the way trimmed-NURBS surfaces are described.

## Acknowledgements

The financial support of the Siemens AG and DAAD (German Academic Exchange Service) for the research is gratefully acknowledged.

## References

[1] C. Song, J. P. Wolf, The scaled boundary finite-element method-alias consistent infinitesim.al finite-element cell method-for elastodynamics, Comput. Methods Appl. Mech. Engrg. 147 (1997) 329–355.

[2] J. P. Wolf, C. Song, The scaled boundary finite-element method - a fundamental solution-less boundary-element method, Comput. Methods Appl. Mech. Engrg. 190 (2001) 5551–5568.

[3] H. Gravenkamp, F. Bause, C. Song, On the computation of dispersion curves for axisymmetric elastic waveguides using the scaled boundary finite element method, Comput. Struct. 131 (2014) 46–55.

[4] C. Song, A matrix function solution for the scaled boundary finite-element equation in statics, Comput. Methods Appl. Mech. Engrg. 193 (2004) 2325–2356.

[5] G. Lin, Y. Zhang, Z. Hu, H. Zhong, Scaled boundary isogeometric analysis for 2d elastostatics, Science China Physics, Mechanics and Astronomy 57 (2014) 286–300.

[6] S. Goswami, W. Becker, Computation of 3-d stress singularities for multiple cracks and crack intersections by the scaled boundary finite element method, Int. J. Fracture 175 (2012) 13–25.

[7] C. Song, J. P. Wolf, The scaled boundary finite-element method: analytical solution in frequency domain, Comput. Methods Appl. Mech. Engrg. 164 (1998) 249–264.

[8] C. Song, J. P. Wolf, The scaled boundary finite-element method–a primer: solution procedures, Comput. Struct. 78 (2000) 211–225.

[9] T. J. R. Hughes, J. A. Cottrell, Y. Bazilevs, Isogeometric analysis: CAD, finite elements, NURBS, exact geometry and mesh refinement, Comput. Meth. Appl. Mech. Engrg. 194 (2005) 4135–4195.

[10] D. Schillinger, J. A. Evans, A. Reali, M. A. Scott, T. J. Hughes, Isogeometric collocation: Cost comparison with galerkin methods and extension to adaptive hierarchical nurbs discretizations, Comput. Methods Appl. Mech. Engrg. 267 (2013) 170–232.

[11] F. Auricchio, L. B. Da Veiga, T. Hughes, A. Reali, G. Sangalli, Isogeometric collocation methods, Math. Mod. Meth. Appl. S. 20 (2010) 2075–2107.

[12] J. P. Wolf, C. Song, The scaled boundary finite-element method–a primer: derivations, Comput. Struct. 78 (2000) 191–210.

[13] C. Song, J. P. Wolf, Body loads in scaled boundary finite-element method, Comput. Methods Appl. Mech. Engrg. 180 (1999) 117–135.